

REVIEW ARTICLE

3D printing and bioprinting in urology

Kun Liu^{1†}, Nan Hu^{2†}, Zhihai Yu¹, Xinzhou Zhang², Hualin Ma^{2*}, Huawei Qu^{3*}, and Changshun Ruan^{3*}¹Department of Urology, Three Gorges Hospital, Chongqing University, Chongqing, China²Department of Nephrology, Shenzhen People's Hospital (The Second Clinical Medical College, Jinan University; The First Affiliated Hospital, Southern University of Science and Technology), Shenzhen, China³Research Center for Human Tissue and Organs Degeneration, Institute of Biomedicine and Biotechnology, Shenzhen Institute of Advanced Technology, Chinese Academy of Sciences, Shenzhen, China**Abstract**

Three-dimensional (3D) printing with highly flexible fabrication offers unlimited possibilities to create complex constructs. With the addition of active substances such as biomaterials, living cells, and growth factors, 3D printing can be upgraded to 3D bioprinting, endowing fabricated constructs with biological functions. Urology, as one of the important branches of clinical medicine, covers a variety of organs in the human body, such as kidneys, bladder, urethra, and prostate. The urological organs are multi-tubular, heterogeneous, and anisotropic, bringing huge challenges to 3D printing and bioprinting. This review aims to summarize the development of 3D printing and bioprinting technologies in urology in the last decade based on the Science Citation Index-Expanded (SCI-E) in the Web of Science Core Collection online database (Clarivate). First, we demonstrate the search strategies for published papers using the keywords such as "3D printing," "3D bioprinting," and "urology." Then, eight common 3D printing technologies were introduced in detail with their characteristics, advantages, and disadvantages. Furthermore, the application of 3D printing in urology was explored, such as the fabrication of diseased organs for doctor-patient communication, surgical planning, clinical teaching, and the creation of customized medical devices. Finally, we discuss the exploration of 3D bioprinting to create *in vitro* bionic 3D environment models for urology. Overall, 3D printing provides the technical support for urology to better serve patients and aid teaching, and 3D bioprinting enables the clinical applications of fabricated constructs for the replacement and repair of urologically damaged organs in future.

[†]These authors contributed equally to this work.

***Corresponding authors:**Hualin Ma
(mahualin0796@sina.com)Huawei Qu
(hw.qu@siat.ac.cn)Changshun Ruan
(cs.ruan@siat.ac.cn)

Citation: Liu K, Hu N, Yu Z, *et al.*, 2023, 3D printing and bioprinting in urology. *Int J Bioprint*, 9(6): 0969. <https://doi.org/10.36922/ijb.0969>

Received: May 21, 2023**Accepted:** July 4, 2023**Published Online:** August 10, 2023

Copyright: © 2023 Author(s). This is an Open Access article distributed under the terms of the Creative Commons Attribution License, permitting distribution, and reproduction in any medium, provided the original work is properly cited.

Publisher's Note: AccScience Publishing remains neutral with regard to jurisdictional claims in published maps and institutional affiliations.

Keywords: 3D printing; Bioprinting; Urology**1. Introduction**

Three-dimensional (3D) printing, also known as additive manufacturing (AM), has been developed and improved over the last few decades^[1-4]. Traditional 3D printing technology uses a planar layer printing strategy with a process originally developed for rapid prototyping. Digital models are sliced by it along the Z-axis to produce a set of digital models with horizontal build layers in the X-Y plane. These layers are then stacked

sequentially from bottom to top to create a physical replica of the digital model. With the reform and innovation of 3D printing technology, several types of 3D printing techniques with different characteristics have been developed, such as the conventional fused deposition modeling (FDM) for hot melt extrusion deposition of polymer materials, digital light processing (DLP) for photo-crosslinking molding, and bioprinting/biofabrication for processing biomaterials and cellular bioink^[2,5,6].

3D bioprinting, also known as biofabrication and biomanufacturing, is developed from 3D printing by adding cells, proteins, growth factors, and biomaterials to the printing ink, and its purpose is to create samples with specific biological functions. The development of 3D bioprinting can be divided into five stages based on the nature of products^[7]: (1) biomedical *in vitro* devices without requiring biocompatibility; (2) biocompatible but non-degradable products; (3) biocompatible, degradable, and absorbable products; (4) cells as ink components; and (5) cellular microspheres and micro-organs^[7]. In this review, we define that 3D printing includes stages 1 to 3, and 3D bioprinting includes stages 4 and 5.

3D printing and bioprinting have been used in a variety of applications including architecture, flexible electronics, tissue engineering (such as bone, meniscus, and blood vessels), and manufacturing of mechanical devices^[8-15]. However, the application of 3D printing and bioprinting in urology is relatively rare^[16-18]. The urological system, as one of the important systems of the body, plays a vital role in maintaining normal life activities. Urological organs are multi-tubular, heterogeneous, and anisotropic. 3D printing and bioprinting, as well as non-traditional subtractive manufacturing methods, offer flexibility in designing and fabricating complex scaffolds. Urological organ damage would directly or indirectly affect human life and health, so it is necessary to explore the potential of 3D printing and bioprinting in addressing urological disorders. Overall, this paper reviews the research progress of 3D printing and bioprinting technology in urology in the past 10 years (2013–2022), covering urological reconstruction models for preoperative planning, surgical teaching, medical devices for sizing customization and reducing medical costs, and tissue-engineered bioscaffolds for mimicking urological organs. It is believed that 3D printing and bioprinting have broader application prospects in urology in the future and have the opportunity to solve urological diseases.

2. Search strategy

All publications used in this study were obtained by performing searches on the Science Citation Index-Expanded (SCI-E) in the Web of Science Core Collection

online database (Clarivate). The searches were conducted to find high-quality articles published in English between January 1, 2013, and December 31, 2022. Three search strategies were conducted for “3D printing” (search strategy #1), “3D printing in urology” (search strategy #2), and “3D bioprinting in urology” (search strategy #3), respectively, as shown in Table 1. These three search strategies yielded only research articles, and other publication types, including review papers, conference papers, conference abstracts, editorial materials, book chapters, etc., were not included unless they overlap with research papers. The topic subject (TS) term “3D printing” and its near-synonyms (such as “three-dimensional printing” and “direct ink writing”) were used to retrieve publications on 3D printing. The TS term “3D bioprinting” and its near-synonyms (such as “biofabrication” and “biomanufacturing”) were used to retrieve publications on 3D bioprinting. The title (TI) and abstract (AB) terms including “urology” and its involved organs including nephrology, prostate, kidney, ureter, bladder, urethra, penile, penis, and “adrenal gland” were placed in the search strategies for urology. This research was conducted following the Preferred Reporting Items for Systematic Reviews and Meta-analyses (PRISMA) statement, as illustrated in Figure 1.

Search results (“3D printing” in search strategy #1) show that, as shown in Figure 2A, 3D printing has received increasing attention and has been widely researched in recent years. Moreover, Figure 2B further demonstrates the level of attention 3D printing has received, by means of the number of highly cited papers in the Essential Science Indicators (ESI) of the Web of Science Core Collection. Other search results (“3D printing and urology” in search strategy #2, Figure 3A; “3D bioprinting in urology” in search strategy #3, Figure 3B) indicate that the research and exploration of 3D printing and bioprinting in urology is increasing. However, the use of 3D printing in the field of urology accounts for only about 1/5000 of its overall use in various fields. There are no highly cited papers on 3D printing in urology. Therefore, the application of 3D printing in urology remains a research gap awaiting to be addressed.

3. Characteristics of various 3D printing technologies

In recent years, the rapid development of 3D printing provides the technological basis for building a bridge between engineering, biology, materials science, and clinical medicine. 3D printing technology is one of the crucial elements of multi-disciplinary integration to solve clinical problems. The working process of 3D printing is shown in Figure 4. First, a target object is scanned by instruments such as micro-computed tomography

Table 1. The search strategies used in this paper and their details

Strategy	Query preview	Publications
"3D printing" (#1)	TS=((("3D" OR "3-D" OR "three dimensional" OR "3-dimensional") AND ("print" OR "fabricat*" OR "manufactur*")) OR "additive manufacturing" OR "stereolithography" OR "fused deposition modeling" OR "selective laser sintering" OR "selective laser melting" OR "powder bed fusion" OR "binder jetting" OR "material extrusion" OR "direct ink writing" OR "material jetting" OR "rapid prototype*" OR "bioprint*" OR "biofabricat*" OR "bioplot*") AND DOP=(2013-01-01/2022-12-31) AND DT=(("ARTICLE"))	105,891
"3D printing" AND "urology" (#2)	TS=((("3D" OR "3-D" OR "three dimensional" OR "3-dimensional") AND ("print*" OR "fabricat*" OR "manufactur*")) OR "additive manufacturing" OR "stereolithography" OR "fused deposition modeling" OR "selective laser sintering" OR "selective laser melting" OR "powder bed fusion" OR "binder jetting" OR "material extrusion" OR "direct ink writing" OR "material jetting" OR "rapid prototype*" OR "bioprint*" OR "biofabricat*" OR "bioplot*") AND ((TI = (urology OR nephrology OR prostate OR kidney OR ureter OR bladder OR urethra OR penile OR penis OR "adrenal gland")) OR (AB = (urology OR nephrology OR prostate OR kidney OR ureter OR bladder OR urethra OR penile OR penis OR "adrenal gland"))) AND DOP=(2013-01-01/2022-12-31) AND DT=(("ARTICLE"))	531
"3D bioprinting" AND "urology" (#3)	TS=((("3D" OR "3-D" OR "three dimensional" OR "3-dimensional") AND ("bioprint*" OR "biofabricat*" OR "biomanufactur*")) OR "direct ink writing" OR "bioprint*" OR "biofabricat*" OR "bioplot*") AND ((TI = (urology OR nephrology OR prostate OR kidney OR ureter OR bladder OR urethra OR penile OR penis OR "adrenal gland")) OR (AB = (urology OR nephrology OR prostate OR kidney OR ureter OR bladder OR urethra OR penile OR penis OR "adrenal gland"))) AND DOP=(2013-01-01/2022-12-31) AND DT=(("ARTICLE"))	73

Booleans: AND, OR, and NOT; TS = topic subject; TI = title; AB = abstract; DOP = publication date; DT = document types.

(micro-CT) or magnetic resonance imaging (MRI). Then, the 3D digital model of the target object is obtained by reconstruction, design, and repair using computer-aided design (CAD) software and exported in STL or IGES file format for subsequent 3D printing. Next, the appropriate 3D printer and printing materials are selected based on the part's purpose and processing accuracy. Finally, the digital model is imported into the 3D printer for fabrication. It is important to note that some printing methods require post-processing for printed samples. 3D printing can be divided into different categories according to its working principle and applicable materials, mainly including stereolithography (SLA)^[19-21], DLP^[2,11,22], FDM^[11,23,24], direct ink writing (DIW)^[25-31] (through which the printed material is a series of lines or droplets), material jetting (MJ)^[32], binder jetting (BJ)^[33-35], selective laser sintering (SLS)^[36,37], and selective laser melting (SLM)^[38-41] (Figure 5). The characteristics, materials, advantages, and disadvantages of these different types of 3D printing technologies are demonstrated in Table 2.

In detail, SLA technology uses an oscillating mirror system to control the ultraviolet (UV) laser (355 nm or 405 nm) spot scanning crosslinking to achieve the curing of resin materials, which has better mechanical properties but less applicable materials, poor processing accuracy, and slow processing speed (Figure 5A). Moreover, the incomplete crosslinked resin is toxic, which is a shortcoming. Based on SLA technology, scientists developed a DLP system based on a digital mirror device and photosensitive polymers liquid, which has high precision and fast fabrication (Figure 5B). Moreover, with the rapid development of DLP, it is able to perform biofabrication of organs and tissues, such as heart and blood vessels, for potential future applications. In contrast to the previous two 3D printing technologies that employ liquids, FDM technology, one of the most widely used 3D printing technologies, utilizes solid polymer wire as the raw material (e.g., polylactic acid [PLA], acrylonitrile butadiene styrene [ABS], poly-ε-caprolactone [PCL]), which is melted by heating and then stacked layer by layer to build 3D-printed samples (Figure 5C). The common heating temperature of this technology is 50–280°C, which can generally melt most of the polymers. PCL, which has been approved by the US Food and Drug Administration (FDA), is used in tissue engineering areas including bone tissue engineering and meniscal tissue engineering. Although this technology is widely used in crafts, polymer parts, tissue engineering scaffolds, etc., its biggest limitation is that it cannot be bioprinted because of its high-temperature molten heating process, which is fatal to cells. DIW technology (Figure 5D) has a great advantage in bioprinting because of its technical simplicity and the wide range of available ink materials, such as hydrogel,

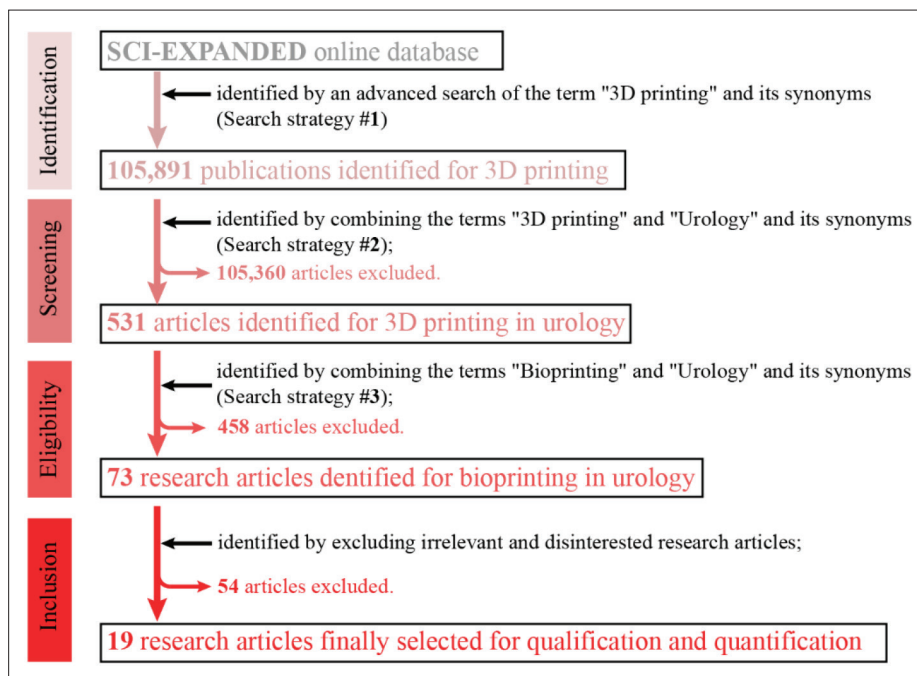


Figure 1. Flow chart of the literature search used in this study based on the Preferred Reporting Items for Systematic Reviews and Meta-analyses (PRISMA) method.

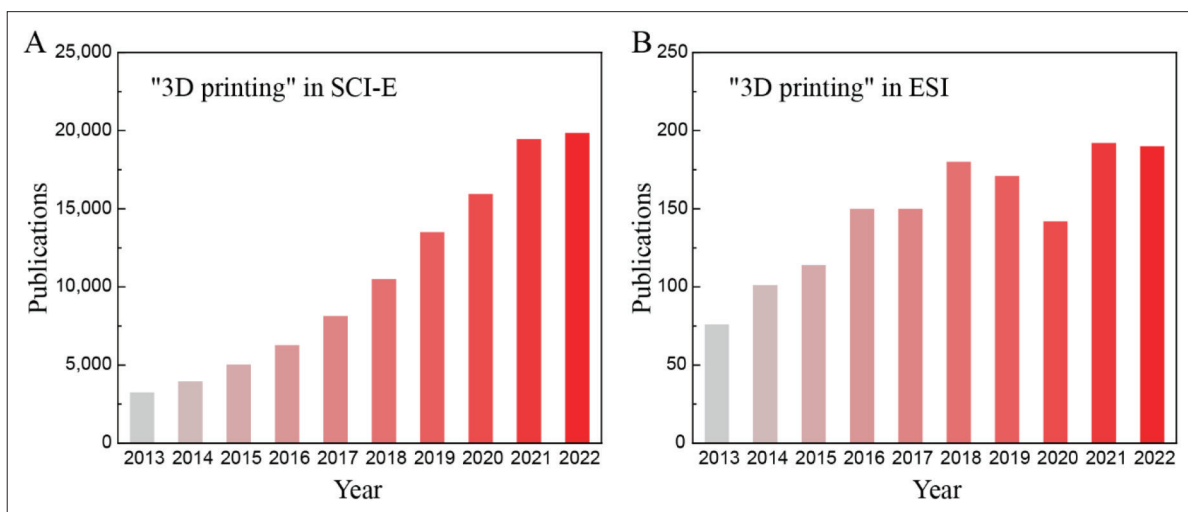


Figure 2. The number of published papers with “3D printing” as the topic subject (TS) term in the Science Citation Index-Expanded (SCI-E) (A) and the Essential Science Indicators (ESI) (B) of the Web of Science Core Collection between January 1, 2013, and December 31, 2022.

gelatin, and gelatin methacryloyl (GelMA), which can be easily printed with live cell ink. The ink extruded from the nozzle can be divided into two states: fiber (Figure 5D-i) and droplet (Figure 5D-ii). The DIW technology with continuous uniform diameter fiber state is widely applied to print various bioink applications. Especially, it has been widely adopted in the last decade for use in research. The greatest advantage of DIW technology is that it allows the biofabrication of widely available materials (various types

of hydrogels) incorporating cells at room temperature, and the greatest disadvantage is the generally poor mechanical properties of the scaffolds obtained. In the future, high-strength hydrogels can be studied in-depth to further develop and popularize the adoption and acceptance of DIW technology in biofabrication. In addition to the DIW technology that uses droplet state, there are two other 3D printing technologies that we know of through droplets, and they are MJ (Figure 5E) and BJ (Figure 5F).

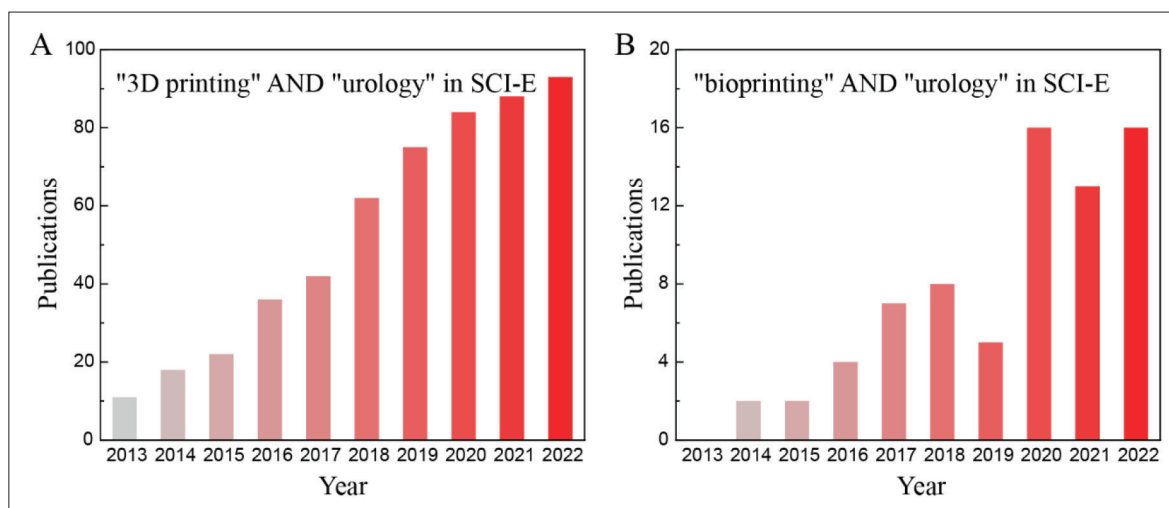


Figure 3. The number of publications with “3D printing” and “urology” (A) and “bioprinting” and “urology” (B) as the topic subject (TS) terms in the Science Citation Index-Expanded (SCI-E) database of Web of Science Core Collection between January 1, 2013, and December 31, 2022.

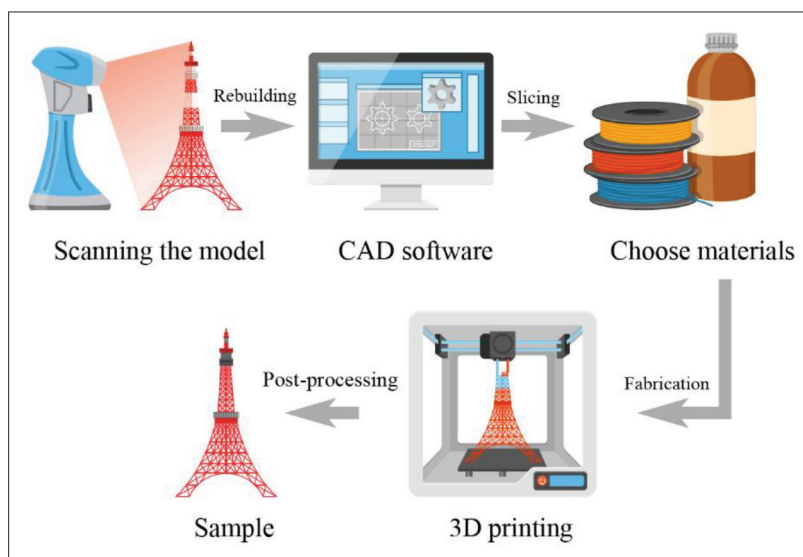


Figure 4. Design and fabrication workflow for 3D printing (Designed with macrovector/Freepik).

The difference between these two technologies is that MJ executes 3D printing by spraying droplet materials (e.g., liquid polymer or metal materials) and then crosslinking them with UV light for polymers or cooling them at room temperature for metal materials (Figure 5E), while BJ executes 3D printing by spraying binder on a bed of granular powder by bonding the particles (Figure 5F). A prominent representative of MJ technology is Stratasys, which has developed a variety of inkjet 3D printers (e.g., J750™ DAP, J8 Series™) that can handle multiple transparent or opaque materials for high-fidelity processing 3D models. The technologies that use powder bed fusion (PBF) are SLS (Figure 5G) and SLM (Figure 5H), which, unlike BJ, employ a laser to selectively heat-specific areas of

powdered granular material for 3D printing. The difference between these two technologies (SLS and SLM) is the laser power used. SLS mainly heats and melts polymer materials with low melting point, which are used as binder to paste ceramic or metal materials (Figure 5G), while SLM uses high power laser to completely melt polymer or metal materials at high temperatures, resulting in higher precision and better mechanical properties, but consuming more energy and reducing processing speed (Figure 5H).

In summary, each 3D printing technology has unique characteristics and specialized applications, and applicable materials vary from method to method, as shown in Figure 5 and summarized in Table 2. Notably, 3D printing has been

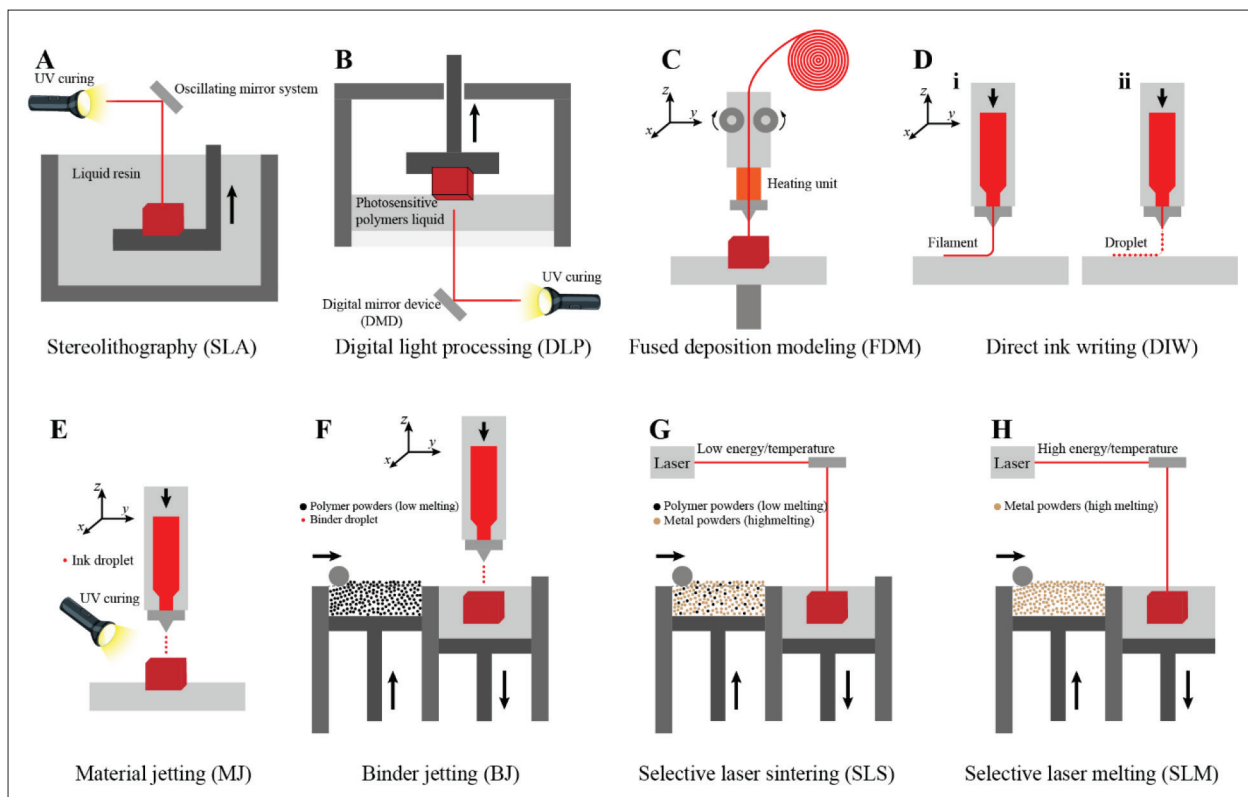


Figure 5. Schematic diagram of different types of 3D printing technologies. (A) Stereolithography (SLA)^[83,84]. (B) Digital light processing (DLP)^[85,86]. (C) Fused deposition modeling (FDM)^[10]. (D) Direct ink writing (DIW)^[28-30]. (E) Material jetting (MJ)^[8]. (F) Binder jetting (BJ)^[34,35]. (G) Selective laser sintering (SLS)^[37,87]. (H) Selective laser melting (SLM)^[38,88,89].

widely explored and applied in many areas, especially in the medical field which has received more attention compared to other fields, as evidenced by the continuous publication of research articles regarding 3D printing in medicine in prestigious journals such as *Nature* and *Science*^[42-47]. The applications in urology can be divided into two main areas: 3D printing and bioprinting. The working environment of the printing method determines whether it is available to process cell-loaded bioinks. Therefore, 3D printing technologies (including SLA, FDM, BJ, SLS, and SLM) are used to process non-cellular urological samples, and 3D bioprinting technologies (including DLP, DIW, and MJ) are used to fabricate biological scaffolds with specific biological functions.

4. Clinical applications of 3D printing in urology

Urological disorders seriously affect human health, some of which can be managed with standard treatments that can alleviate patient suffering, but many are in dire need of new therapeutic strategies. Based on some studies, 3D printing gives a silver lining in tackling certain diseases that can be addressed with the use of tissue engineering, particularly

those related to bone and cartilage^[9], and it is believed that 3D printing can make a difference in urology in the future. 3D printing has gained wide interest in different fields due to its high application flexibility in many areas, including aerospace, automotive, food, architecture, batteries, flexible sensors, robotics, etc. The application of this technology in urology could be mainly divided into preoperative planning, surgical simulation, and preclinical application.

4.1. Preoperative planning

3D-printed urological models can facilitate interactions, including preoperative doctor-patient communication, surgical planning, and clinical teaching. To improve the accuracy of robot-assisted radical prostatectomy (RARP) surgery, Saba *et al.* reconstructed a digital model (Figure 6A-ii) of the prostate lesion site based on the patient's prostate MRI data (Figure 6A-i) and obtained the 3D-printed model (Figure 6A-iii) before the surgery^[48]. The results demonstrated that the preoperative 3D-printed sample could provide urologists with more accurate and effective information for RARP surgery compared to continuous 2D MRI data, as shown in Figure 6A. Chandak *et al.* employed 3D printing to assist in the understanding of RARP surgery, indicating that visualization via 3D

Table 2. A summary of the characteristics, materials, advantages, and disadvantages of various 3D printing technologies

Method	Characteristic	Material	Advantage	Disadvantage	Ref.
SLA	UV crosslinking of photosensitive liquid resin to solid by laser beam	Photosensitive liquid resin	High mechanical properties, high resolution, and the ability to process large sizes	Toxic, trouble cleaning, less applicable materials, poor processing accuracy	[19-21]
DLP	Second-generation light-curing technology based on projector curing of photosensitive materials	Photosensitive polymer liquid, hydrogel	High mechanical properties, high resolution, faster processing speed, and bioprinting	Limited materials available	[2,11,22]
FDM	Wire material is heated at high temperature and then extruded	Polymers or composites	High mechanical properties and the ability to process large sizes	High temperature	[11,23,24]
DIW	Extrusion of viscoelastic materials for stacking and molding	Various materials (e.g., GelMA)	A wide range of available materials, room temperature, and bioprinting	Low mechanical strength	[25-31]
MJ	Liquid materials (droplets or lines) are sprayed and stacked.	Organic solutions and polymers	High resolution	Organic reagents or high temperature	[32]
BJ	The binder is injected into the powder bed to bond the pellets into shape	Particles and composites	A wide range of available materials	Low mechanical strength and low resolution	[33-35]
SLS	Sintering powder compacts using a laser as a heat source	Metal, ceramics, and composites	Sintering of powder billets with various materials	High temperature, complex process, and high cost	[36,37]
SLM	Melting and stacking of metallic materials using laser as a heat source	Metal and composites	High mechanical properties and metallic materials	High temperature, complex process, and high cost	[38-41]

Abbreviations: BJ, binder jetting; DIW, direct ink writing; DLP, digital light processing; FDM, fused deposition modeling; GelMA, gelatin methacryloyl; MJ, material jetting; SLA, stereolithography; SLM, selective laser melting; SLS, selective laser sintering.

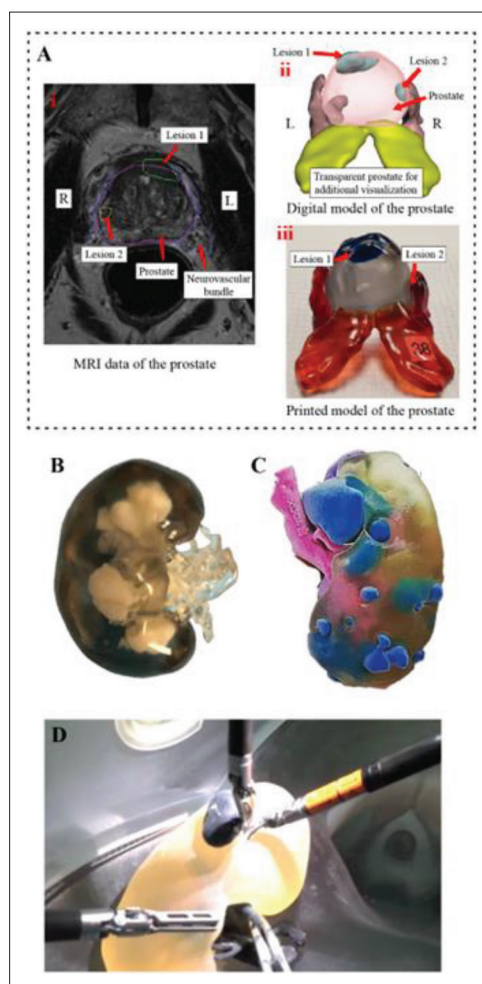


Figure 6. 3D-printed urological kidney models for enhancing interactions and surgical simulation. (A) MRI data (i), reconstructed digital model (ii) and 3D-printed sample (iii) of the diseased prostate^[48]. Reprinted with permission from ref.^[48]. Copyright 2021 Elsevier. (B) A kidney with antler-shaped stones^[51]. (C) A kidney with Von Hippel-Lindau syndrome^[51]. (D) A kidney silicone sample for surgical training^[51]. Reprinted with permission from ref.^[51]. Copyright 2019 Elsevier.

means for simulation is more effective than using only 2D flat data^[49]. The use of 3D-printed prostate models can achieve better understanding than the current gold-standard multi-disciplinary team meetings (MDT) sessions, providing medical students and clinicians with better guidance on surgical positioning^[50].

Further, researchers have conducted 3D printing of kidneys to facilitate doctor-patient communication and clinical teaching^[51]. Researchers from the University of California Irvine (USA) printed kidney samples with antler-shaped stones for preoperative planning (Figure 6B)^[51]. Researchers from Camargo Cancer Center (Brazil) printed diseased kidneys for doctor-patient communication and preoperative planning (Figure 6C)^[51]. 3D printing offers

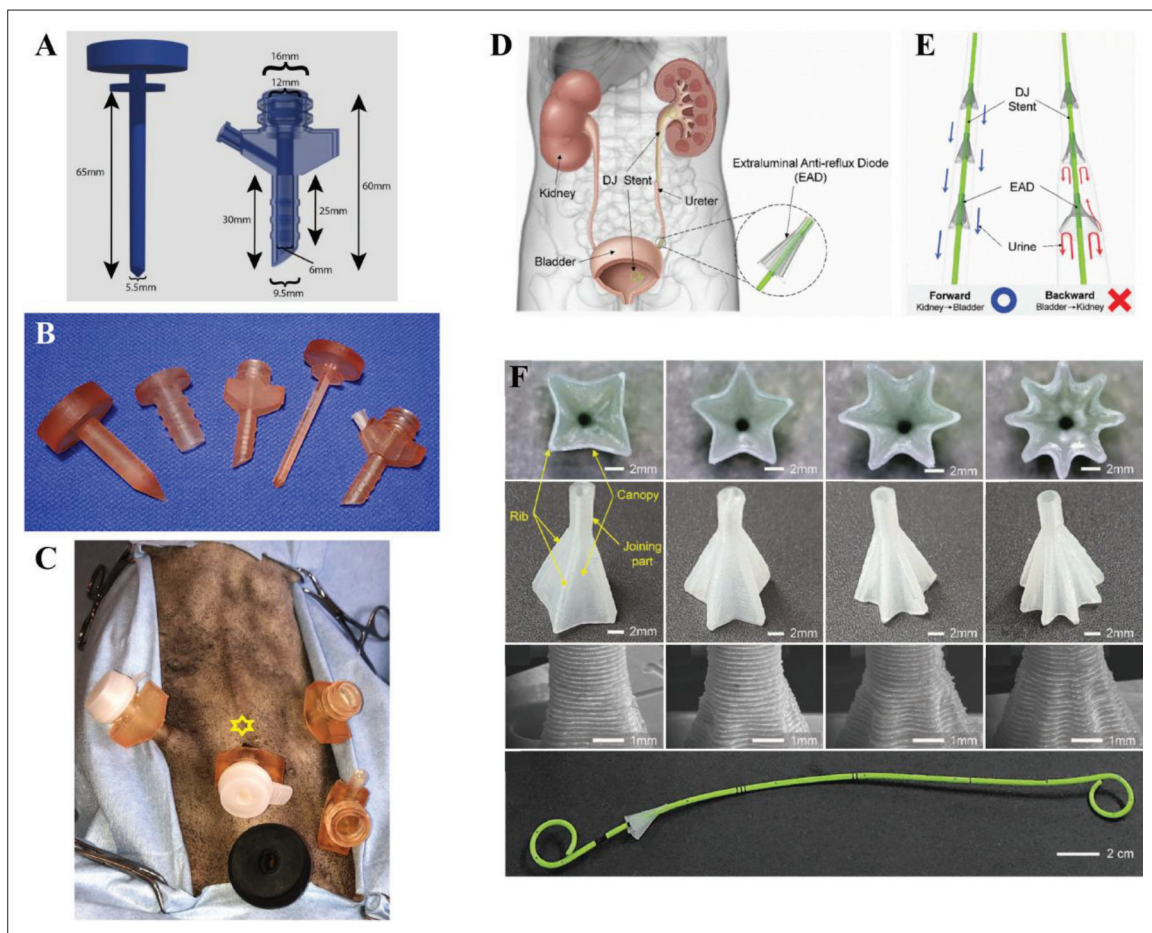


Figure 7. Design and fabrication of the laparoscopic trocar^[90] and extraluminal anti-reflux diodes^[55]. (A) Drawing of cannula and trocar. (B) 3D-printed cannulas. (C) Photograph of the cannula after surgery. Reprinted with permission from ref.^[90]. Copyright 2022 John Wiley and Sons. (D) Schematic diagram of the extraluminal anti-reflux diode (EAD) in urinary organs. (E) Working principle of the EAD. (F) 3D-printed EADs with different shapes. (E) Working principle. (F) Different shapes. Reprinted with permission from ref.^[55] under the Creative Commons Attribution 4.0 International License.

the opportunity and convenience for *in vitro* visualization of diseased urological organs, and its application in urology is expected to significantly facilitate doctor–patient communication and reduce the current doctor–patient conflicts in China due to miscommunication.

4.2. Surgical simulation

Researchers from the University of California Irvine (USA) printed a silicone kidney sample for surgical training (Figure 6D)^[51]. This provides samples for *in vitro* anatomy learning and surgical simulation. In addition, other researchers have developed a 3D-printed kidney simulation platform. It can be used by urologists for rehearsal testing before formal surgery for kidney tumor removal. In the rehearsal, the surgeon is allowed to use various methods to remove the tumor and examine the model after each simulation and thus modify the surgical plan accordingly. The 3D-printed models effectively simulated the texture, anatomy, and perfusion of the kidney, providing a platform

for a fully immersive experience in conducting a surgery. As shown in Figure 6E, the actual surgery and simulated images are displayed on the left and right, respectively^[52]. In summary, the application of 3D printing in urology can help improve urologists' surgical skills, enhance surgical protocols, increase surgical success, and predict surgical outcomes based on model simulation results.

4.3. Preclinical application

Here, some applications of 3D-printed medical devices for urology were reported. del Junco *et al.* designed and fabricated laparoscopic punctures and ureteral stents using CAD software and 3D printing technology, and *in vivo* puncture experiments in pigs showed that the resulting devices are feasible and could be used in clinical settings in the future^[53]. Buote *et al.* created and trained a variety of 3D-printed PLA scaffolds, and the surgical results showed that the use of their stents was successful, and there were no postoperative complications (Figure 7A–C)^[90]. Further,

Park *et al.* fabricated a polymeric anti-reflux flap valve via 3D printing technology, which can be attached to a ureteral stent and can effectively resist reflux^[54]. To improve anti-reflux, Lee *et al.* created extraluminal anti-reflux diodes with various shapes, which can be used in ureteral stents^[55], as shown in Figure 7D–F.

5. 3D bioprinting in urology

3D bioprinting is commonly defined as the process of fabricating cell-loaded biological materials into tissue-engineered scaffolds. Although 3D printing provides technical support for the construction of urological tissue-engineered scaffolds with similar shapes, only 3D bioprinting can endow them with biological functions by incorporating biomaterials, live cells, and growth factors. The essence of bioprinting is the processing of living cells, which requires that the whole process of 3D printing should be friendly or non-invasive to living cells. Common 3D bioprinting technologies include extrusion-based bioprinting (single-, multi-, and coaxial-nozzle), inkjet-based bioprinting (piezoelectric and thermal), and light-based bioprinting (UV light and laser light)^[13]. Although current technologies are not feasible to reconstruct organs *in vitro* that are fully capable of normal human activity for clinical transplantation, 3D bioprinting offers the possibility to reconstruct biologically active and functional urological organs.

Our search revealed a total of 73 research papers on bioprinting in urology based on search strategy #3. Of these, 19 research articles were selected for detailed study^[56–74] (as shown in Table 3) after excluding literature reported works that used only urological cells, or some review articles that were incorrectly categorized as research article. Among these articles, 11 are about the kidney^[56–58,62,63,65,67,69–72], 6 about the bladder^[59–61,64,66,73], 1 about the glomerular^[68], and 1 about the urinary tract^[74]. Of these papers, extrusion bioprinting is the most widely used 3D bioprinting technology, due to its advantages such as low device cost, a wide range of applicable materials, and cell-friendliness. To present the advances of 3D bioprinting in urology, we divide this section into four parts: bioinks, cell types, structure design, and urological scaffolds, as shown in Figure 8.

5.1. Bioinks

Bioink is the raw material for 3D bioprinting, which is processed into samples according to the structure design with the aid of printing equipment. Currently, there are various formulations of bioink, which is mainly composed of basic biomaterials and bioadditives. The 3D bioprinting method determines the type of basic biomaterial required. The commonly used biomaterials include natural and synthetic materials. Generally, natural materials have

excellent biocompatibility, but their mechanical properties are poor compared to synthetic materials. The popular biomaterials are mainly hydrogels, gelatin, alginate, decellularized extracellular matrix (dECM), and their mixtures. As the most widely used synthetic material in 3D bioprinting^[75–79], hydrogel can mimic the extracellular matrix (ECM) and provide a physiologically similar environment for cell growth. Gelatin, alginate, and dECM are acceptable natural materials. The basic biomaterials provide carriers for the placement of live cells, and they can undergo biological reactions. Viscoelastic bioinks are usually processed using an extrusion strategy and can be handled equally well using a light-curing strategy by adding a photoinitiator.

5.2. Cell types

Bioprinting revolves around the processing and manufacturing of cell-loaded bioink. The cells represent one of the keys to bioprinting, and their selection endows the sample with specific functions. To mimic the biological microenvironment of natural urological organs *in vitro* as much as possible, cells from the target organ, such as human urothelial cells (HUCs) from urinary tract^[74], human renal progenitor cells (hRPCs) and human embryonic kidney 293 cells (HEK293) from the kidney^[63], human bladder smooth muscle cells (HBSMCs) and T24 cell from bladder^[59,60], are usually used, according to the reviewed literature. In addition, stem cells are one of important cells for 3D bioprinting in urology due to their ability to differentiate into other cells, such as human bone marrow-derived mesenchymal stem cells (hBMSCs)^[61].

5.3. Structure design

The printing method determines the strategy of structure design and the type of bioinks. The most widely accepted 3D bioprinting technology is the extrusion strategy, which relies on bioink deposition to form fibers to build the sample layer by layer. In addition, the extrusion strategy is carried out with the help of a three-coordinate printer or a six-degree-of-freedom robot arm to control the nozzle movement, and the viscoelastic bioink extrusion is achieved by screw, pneumatic, or piston.

According to the fluid process of the ink flow through the nozzle, we can get $D = 2 \times (Q/\pi v)^{0.5}$, where D , Q , and v are the ideal diameter of the fiber, bioink flow, and printing speed, respectively^[80]. It can be obtained that there is a functional relationship between the printing speed and the ideal diameter of the deposited fibers. Specifically, with a fixed print head size and printing parameters, the printing speed determines the size of the ideal diameter of the fiber and the printability of the bioink. During 3D bioprinting, a very high printing speed will result in fiber breakage and discontinuity, while a very low speed will

Table 3. A summary of 3D bioprinting in urology

Year	Urological organ	3D printing technology	Material	Cell	Discovery/Achievement	Ref.
2022	Kidney	Coaxial extrusion printing	Polyethylene vinyl acetate (PEVA)	HK-2s, Caco-2s, and GE cells	Building a secondary hyperoxaluria model	[56]
2022	Kidney	DoD bioprinting	Fibrinogen, alginate	Induced renal tubular epithelial cells (IRECs)	Building a biomimetic 3D microenvironment modeling for polycystic kidney disease	[57]
2022	Renal glomerulus	Coaxial extrusion printing	PICO, and POMaC	HUVECs	Building a series of micro-scale tube channels with biomic shapes	[58]
2022	Bladder	Microfluidic	PDMS	T24 cell	Building a bladder cancer microenvironment	[59]
2022	Bladder	Microfluidic	PDMS	T24 cell	Building a chip-based non-muscle-invasive bladder cancer model	[60]
2022	Bladder	Extrusion printing	Bladder tissue-derived dECM (BdECM)	hBMSCs	Building a bladder model with a bionic structure	[61]
2022	Kidney	Multi-nozzle extrusion printing	Gelatin, and sodium alginate	HEK293, EK293-GFP, and Human kidney fibroblasts	Building a kidney cancer model for drug detection	[62]
2021	Kidney	Extrusion printing	dECM	hRPCs	Building a renal 3D microenvironment	[63]
2021	Bladder	Extrusion printing and microfluidic	GelMA	T24, 5637, MRC-5, and THP-1 cells	Building a bladder cancer microarray via microfluidic	[64]
2021	Kidney	DoD bioprinting, self-assembly technology	Matrigel and Collagen I, and Matrigel-Collagen I blends	Renal PTECs, TERT1, #CRL-4031	Building controllable renal spheroids and nephron-like tubules	[65]
2021	Bladder	Extrusion printing and microfluidic	DMEM	NOR-10 fibroblast cells, and uroepithelial cells	Developing a highly concentrated fibroblast platform to construct bladder-like organs	[66]
2021	Kidney	Extrusion printing	STEMdiff APEL or TESR-E6 medium prior	Human pluripotent stem cells (hPSCs)	Developing a technique for high-throughput extrusion printing of kidney-like organs in well plates	[67]
2020	Renal glomerulus	Microfluidic	Hydrogel	Endothelial cell	Developing bionic kidney glomeruli with complex concave and convex morphology	[68]
2019	Kidney	Extrusion printing	Bacterial nanocellulose, and alginate	HUVECs	Developing a microchannels	[69]
2019	Kidney	Extrusion printing	dECM, gelatin, HA, and glycerol	Human primary kidney cells	Developing a renal bioscaffold using dECM	[70]
2019	Kidney	Extrusion printing, sacrificial template, and microfluidic	Gelatin and fibrinogen	Human immortalized PTECs (RPTEC/TERT1; ATCC CRL4031)	Developing a kidney scaffold for kidney function, disease modeling, and pharmacology	[71]
2019	Kidney	Electrospinning	PCL	ciPTECs	Building a kidney tubule scaffold	[72]
2018	Bladder	Extrusion printing	DMEM	Bone marrow-derived cells	Building functional urinary bladders	[73]
2018	Urinary tract	Coaxial extrusion printing	GelMA, alginate, and PEGOA	HUCs and HBSMCs, HUVECs and HSMCs	Building cannular urothelial tissue constructs and vascular tissue constructs	[74]

Abbreviations: ciPTECs, conditionally immortalized proximal tubule epithelial cells; dECM, decellularized extracellular matrix; DMEM, Dulbecco's modified Eagle's medium; DoD, drop-on-demand; GelMA, gelatin methacryloyl; hBMSCs, human bone marrow-derived mesenchymal stem cells; HBSMCs, human bladder smooth muscle cells; HEK293, human embryonic kidney 293 cells; hRPCs, human renal progenitor cells; HSMCs, human smooth muscle cells; HUVECs, human umbilical vein endothelial cells; HUVECs, human umbilical vein endothelial cells; PCL, poly-ε-caprolactone; PDMS, polydimethylsiloxane; PICO, poly(titaconate-co-citrate-co-octanediol); POMaC, poly(octanediol-co-maleic anhydride-co-citrate); PTECs, renal proximal tubule epithelial cells.

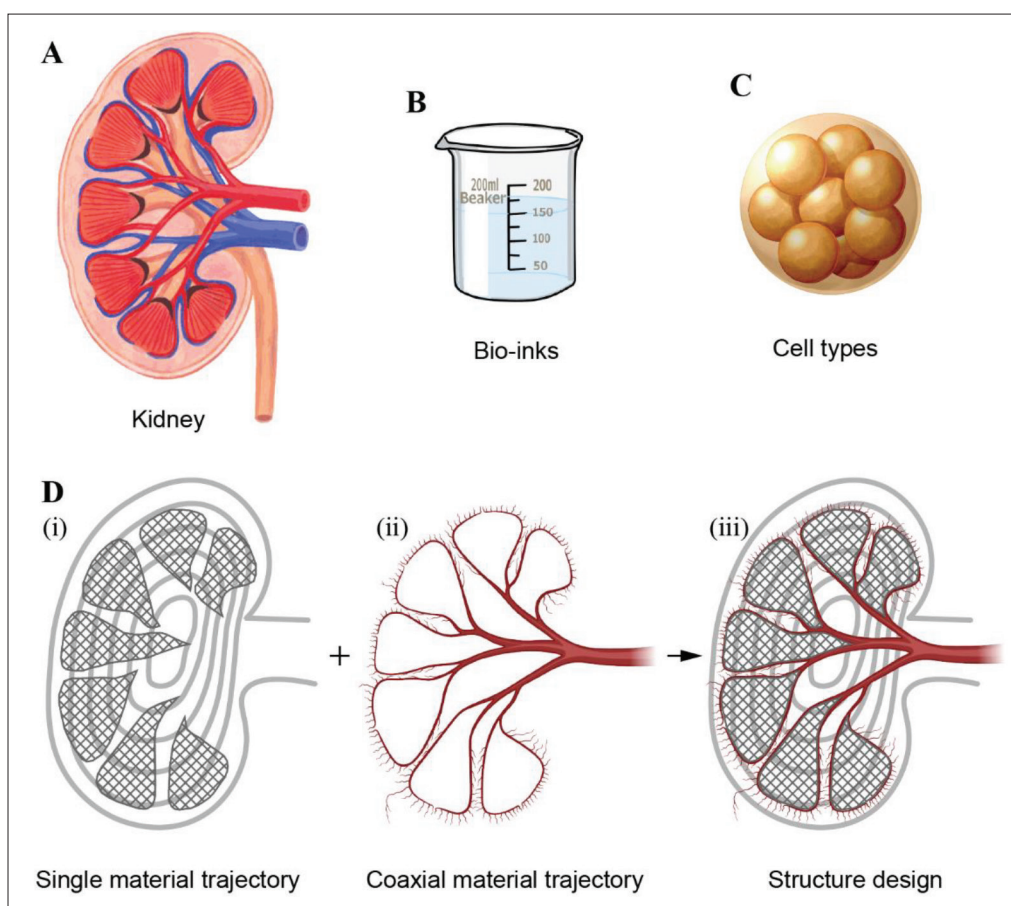


Figure 8. Key factors for 3D bioprinting in urology: (A) design and bioprinting of a kidney scaffold, (B) bioinks, (C) cell types, and (D) structure design.

result in serious ink accumulation and make it difficult to achieve high-fidelity manufacturing of large-size samples. Accurate control of extrusion air pressure is one of the keys to ensuring the survival rate of bioprinted cells; if the air pressure is set too high, it will result in the cells receiving large shear stresses and dying. The use of low extrusion pressure requires hydrogel bioinks with low shear thinning properties. In addition, the innovation of nozzle structure also provides new ideas and inspiration for structural design. Specifically, single nozzle is the most widely used in extrusion printing and can handle one bioink^[81]. Developed from single-nozzle printing^[3], multi-nozzle extrusion printing technology can utilize multiple bioinks and enable to mimic the multi-material and multi-cellular composition of natural urological organs. Coaxial-nozzle printing allows a single nozzle to print two bioinks^[75,82], where the core and shell are usually the sacrificial and scaffold body materials, respectively. It is particularly suitable for the fabrication of tubular samples, such as blood vessels within the kidney, as shown in Figure 8C-ii. The goal of bioprinting is to mimic one or more of the biological functions of a urological organ *in vitro* as much

as possible. As illustrated in Figure 8, which shows the kidney bioprinting process, the blood vessels of varying diameter are expected to mimic the vascular distribution within the kidney and provide structural mimicry for achieving reabsorption in an *in vitro* kidney model.

5.4. Urological scaffolds

The kidneys, ureter, bladder, and urethra together constitute the urinary system of the body, and they are also the organs mainly involved in urology. The kidneys are paired lentil-shaped organs and are one of the important organs of the body, whose basic function is to remove metabolic products from the body. The kidneys are one of the key representatives of bioprinted urological organs. We conclude that the stages of bioprinting development of urological organs, using the kidneys as an example, can be divided into three stages: (1) realization of simple physical and mechanical properties, such as urination of the kidney; (2) replacement, repair, and reconstruction of the kidney urethra; and (3) multi-cellular bionic kidneys with multiple biological functions. Lawlor *et al.* conducted extrusion bioprinting of kidney organoid samples using human pluripotent stem cells (hPSCs) with

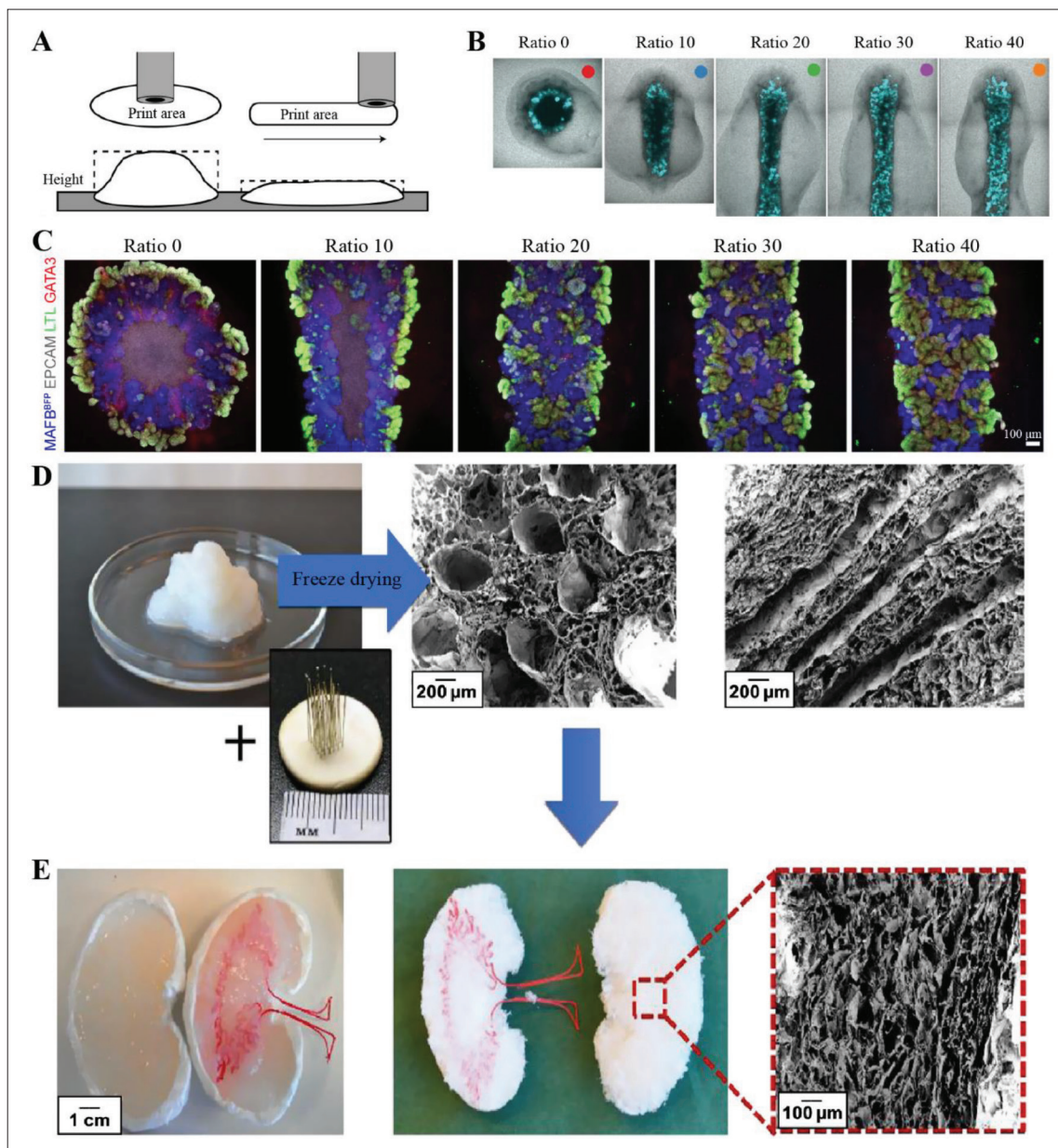


Figure 9. High-throughput extrusion bioprinting of kidney organoids holding promise for drug screening, disease modeling, and kidney organ transplantation (A–C)^[67], and extrusion and sacrificial template method (D, E)^[69]. (A) Schematic diagram of extruded samples at different nozzle movement speeds. (B) Fluorescence imaging of printed samples at different print speeds using MAFB^{mTagBFP2} reporter line. (C) Immunofluorescence of printed samples. Reprinted with permission from ref.^[67]. Copyright 2020 Springer Nature. (D) Freeze-casting method for the fabrication of porous structures. (E) Kidney scaffolds with vascular-like channels. Reprinted with permission from ref.^[69] under the Creative Commons Attribution 3.0 International License.

targeted differentiation, offering promise for drug screening, disease modeling, and kidney organ transplantation (Figure 9A–C)^[67]. They also found that tissue thickness could be precisely controlled by varying the ink extrusion rate and nozzle movement speed (Figure 9A and B), and the results showed that organoids with elongated lengths had a larger total glomerular area than small and thick ones stained by the MAFB gene promoter (MAFB^{mTagBFP2}) reporter

line (Figure 9C)^[67]. Sämfors *et al.* designed and fabricated kidney scaffolds with interconnected macro porosity and vascular-like structures using extrusion printing and sacrificial template method (Figure 9D and E)^[69]. Blood vessels play a vital role in the proper functioning of the body's organs, providing nutrients and oxygen for cellular activity and transporting waste products. Therefore, it is particularly important to construct vascular channels

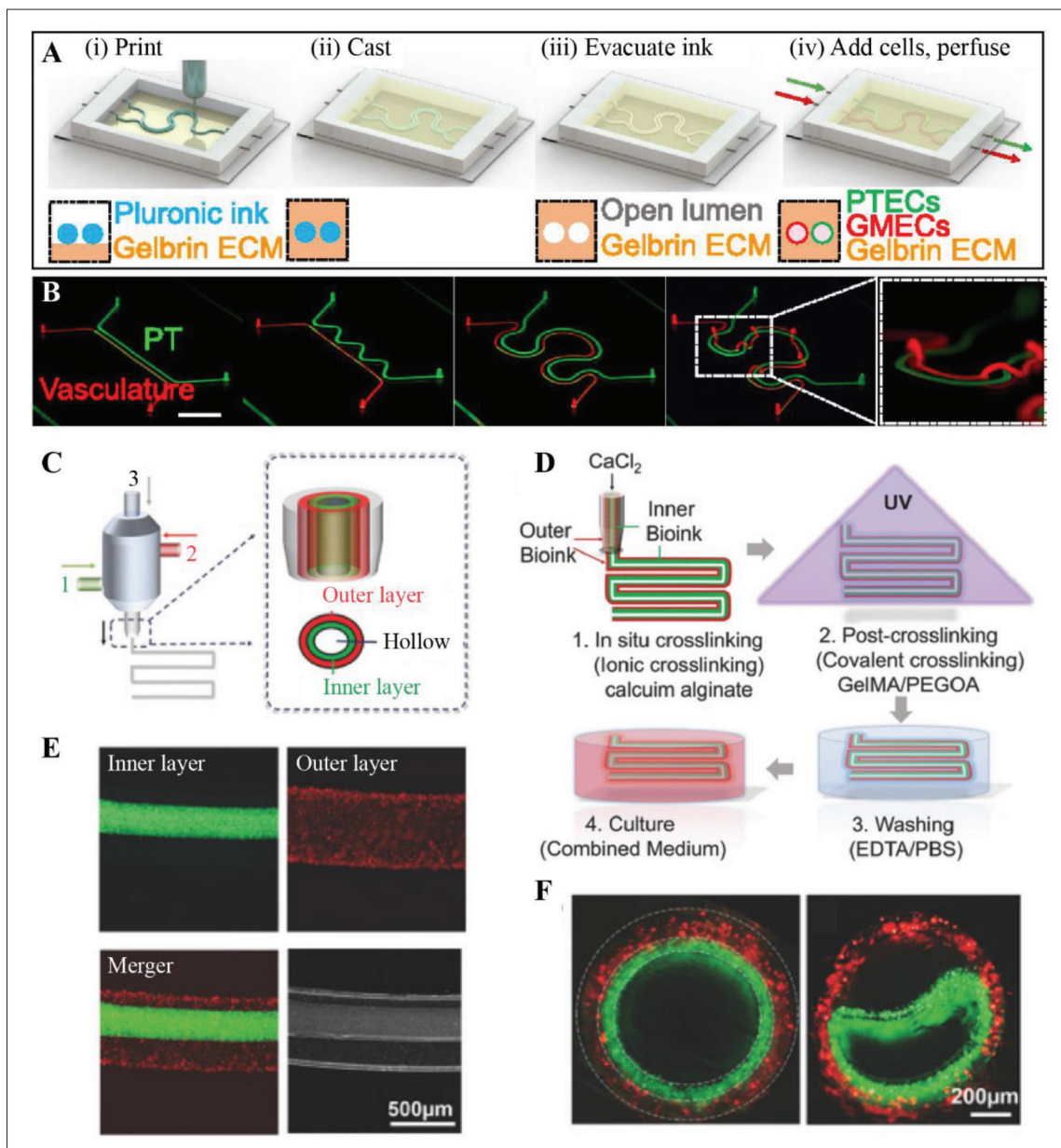


Figure 10. Design and fabrication of vascular samples by single-nozzle extrusion printing and sacrificial template method (A, B)^[74], and coaxial-nozzle extrusion printing (C–F)^[74]. (A) Flow chart of sample fabrication. (B) Vascular samples with different patterns. Reprinted with permission from ref.^[71] under the Creative Commons Attribution 4.0 International License. (C) Schematic diagram of coaxial-nozzle structure. (D) Flow chart of tubular scaffold fabrication. (E) Top and (F) cross-sectional views of stained images of tube samples (green, inner layer; red, outer layer). Reprinted with permission from ref.^[74]. Copyright 1999–2023 John Wiley & Sons.

in 3D-bioprinted urological tissue scaffolds. Lin *et al.* prepared complex vascular patterns using single-nozzle extrusion 3D printing and then obtained vascular channels by sacrificial template method (Figure 10A and B)^[71]. Their results showed that the obtained vascular channels exhibited active reabsorption of albumin and glucose over time, providing a 3D platform for studying kidney function. In addition, Pi *et al.* designed and fabricated annular multi-layer tubular samples by coaxial-nozzle printing technology

(Figure 10C–F)^[74]. Their proposed coaxial nozzle has three inlets, which are the central material, inner layer material, and outer layer material from inside to outside (Figure 10C). The fabricated triple-layer samples are UV-crosslinked and cleaned to obtain a bilayer material tube scaffold with a hollow structure (Figure 10E). This proposed coaxial strategy conceived by Pi *et al.*^[74] provides new insights into the design and fabrication of tubular tissues such as ureters and urethra.

6. Conclusion and outlook

In this review, we summarize the applications of 3D printing and bioprinting in urology. 3D printing of diseased urological organs effectively facilitates doctor-patient communication, preoperative planning, and surgical teaching in urology. Furthermore, 3D printing provides urologists with custom-sized medical devices and reduces medical costs. 3D bioprinting offers new insights for creating urological tissue-engineered scaffolds from biomaterials, living cells, and growth factors. In conclusion, the integration of 3D printing and bioprinting with urology offers new ideas and dynamics for urologists and patients.

In the future, for 3D printing and bioprinting in urology, the following five directions should be explored in-depth:

- (i) Novel 3D printing. Currently, extrusion printing is one of the most widely used technologies for 3D printing and bioprinting. The development of new 3D printing technology is expected to significantly boost fabrication speed and accuracy, sample mechanical properties, and multi-material printing.
- (ii) Novel structures. Urological organs have a complex structure (e.g., kidneys with vessels of varying diameter). The pore structure can facilitate the growth of blood vessels in tissue regeneration. Based on the characteristics of 3D printing technology and materials, the development of new bionic structures is a topic worthy of research.
- (iii) Novel biomaterials. Biomaterials are the primary matter for 3D printing and bioprinting. Newly formulated materials can hopefully promote the development of 3D printing and bioprinting in tissue engineering, including urology.
- (iv) Novel bioadditives. Bioadditives are drug triggers (such as live cells, growth factors, mRNA) for tissue regeneration and repair and can initiate and accelerate biological processes.
- (v) How to balance 3D printing and bioprinting, biomimetic structures, biomaterials, and bioadditives to obtain urological organ scaffolds with near-natural biological functions is a tricky problem.

Acknowledgments

None.

Funding

This work was supported by the National Key R&D Program (Grant No. 2018YFA0703100), the National Natural Science Foundation of China (Grant No. 32122046), the Youth Innovation Promotion Association

of CAS (Grant No. 2019350), the China Postdoctoral Science Foundation (Grant No. 2023M733668), the Guangdong Basic and Applied Basic Research Foundation (2020A1515111190), the Shenzhen Fundamental Research Foundation (JCYJ20210324113001005), the Shenzhen Governmental Sustainable Development Fund (KCXFZ20201221173612034), the Shenzhen Key Laboratory of Kidney Diseases (ZDSYS201504301616234), and the Shenzhen Fund for Guangdong Provincial Highlevel Clinical Key Specialties (No. SZGSP001).

Conflict of interest

The authors declare no conflicts of interests.

Author contributions

Conceptualization: Huawei Qu, Changshun Ruan

Methodology: Kun Liu, Nan Hu, Zhihai Yu, Hualin Ma

Investigation: Kun Liu, Nan Hu, Xinzhou Zhang, Hualin Ma

Writing – original draft: Kun Liu, Huawei Qu

Writing – review & editing: Hualin Ma, Huawei Qu, Changshun Ruan

Supervision: Zhihai Yu, Xinzhou Zhang, Changshun Ruan

Funding acquisition: Xinzhou Zhang, Hualin Ma

Ethics approval and consent to participate

Not applicable.

Consent for publication

Not applicable.

Availability of data

Not applicable.

References

1. Walker DA, Hedrick JL, Mirkin CA, 2019, Rapid, large-volume, thermally controlled 3D printing using a mobile liquid interface. *Science*, 366(6463): 360.
<https://doi.org/10.1126/science.aax1562>
2. Ligon SC, Liska R, Stampfl J, *et al.*, 2017, Polymers for 3D printing and customized additive manufacturing. *Chem Rev*, 117(15): 10212–10290.
<https://doi.org/10.1021/acs.chemrev.7b00074>
3. Skylar-Scott MA, Mueller J, Visser CW, *et al.*, 2019, Voxlated soft matter via multimaterial multinozzle 3D printing. *Nature*, 575(7782): 330–335.
<https://doi.org/10.1038/s41586-019-1736-8>
4. Ouyang L, Armstrong JPK, Lin Y, *et al.*, 2020, Expanding and optimizing 3D bioprinting capabilities using complementary network bioinks. *Sci Adv*, 6(38): eabc5529.

- <https://doi.org/10.1126/sciadv.abc5529>
5. Bandyopadhyay A, Traxel KD, Bose S, 2021, Nature-inspired materials and structures using 3D Printing. *Mater Sci Eng R-Rep*, 145(2021): 100609.
<https://doi.org/10.1016/j.mser.2021.100609>
 6. Qu HW, Fu HY, Han ZY, *et al.*, 2019, Biomaterials for bone tissue engineering scaffolds: A review. *RSC Adv*, 9(45): 26252–26262.
<https://doi.org/10.1039/C9RA05214C>
 7. Sun W, Starly B, Daly AC, *et al.*, 2020, The bioprinting roadmap. *Biofabrication*, 12(2): 022002.
<https://doi.org/10.1088/1758-5090/ab5158>
 8. Qu HW, 2020, Additive manufacturing for bone tissue engineering scaffolds. *Mater Today Commun*, 24(101024): 1–16.
<https://doi.org/10.1016/j.mtcomm.2020.101024>
 9. Qu H, Han Z, Chen Z, *et al.*, 2021, Fractal design boosts extrusion-based 3D printing of bone-mimicking radial-gradient scaffolds. *Research*, 2021(2021): 9892689.
<https://doi.org/10.34133/2021/9892689>
 10. Chatterjee K, Ghosh TK, 2020, 3D printing of textiles: Potential roadmap to printing with fibers. *Adv Mater*, 32(4): 1902086.
<https://doi.org/10.1002/adma.201902086>
 11. Lai J, Wang C, Wang M, 2021, 3D printing in biomedical engineering: Processes, materials, and applications. *Appl Phys Rev*, 8(2): 021322.
<https://doi.org/10.1063/5.0024177>
 12. Yang Y, Xu R, Wang C, *et al.*, 2022, Recombinant human collagen-based bioinks for the 3D bioprinting of full-thickness human skin equivalent. *Int J Bioprint*, 8(4): 611.
<https://doi.org/10.18063/ijb.v8i4.611>
 13. Wu Y, Li M, Su H, *et al.*, 2023, Up-to-date progress in bioprinting of bone tissue. *Int J Bioprint*, 9(1): 628.
<https://doi.org/10.18063/ijb.v9i1.628>
 14. Gao F, Xu ZY, Liang QF, *et al.*, 2019, Osteochondral regeneration with 3D-printed biodegradable high-strength supramolecular polymer reinforced-gelatin hydrogel scaffolds. *Adv Sci*, 6(15): 12.
<https://doi.org/10.1002/advs.201900867>
 15. Lin ZF, Wu MM, He HM, *et al.*, 2019, 3D printing of mechanically stable calcium-free alginate-based scaffolds with tunable surface charge to enable cell adhesion and facile biofunctionalization. *Adv Funct Mater*, 29(9): 1808439.
<https://doi.org/10.1002/adfm.201808439>
 16. Chen MY, Skewes J, Desselle M, *et al.*, 2020, Current applications of three-dimensional printing in urology. *BJU Int*, 125(1): 17–27.
<https://doi.org/10.1111/bju.14928>
 17. Agung NP, Nadhif MH, Irdam GA, *et al.*, 2021, The role of 3D-printed phantoms and devices for organ-specified appliances in urology. *Int J Bioprint*, 7(2): 333.
<https://doi.org/10.18063/ijb.v7i2.333>
 18. Colaco M, Igel DA, Atala A, 2018, The potential of 3D printing in urological research and patient care. *Nat Rev Urol*, 15(4): 213–221.
<https://doi.org/10.1038/nrurol.2018.6>
 19. Ngo TD, Kashani A, Imbalzano G, *et al.*, 2018, Additive manufacturing (3D printing): A review of materials, methods, applications and challenges. *Compos B Eng*, 143(2018): 172–196.
<https://doi.org/10.1016/j.compositesb.2018.02.012>
 20. Mondschein RJ, Kanitkar A, Williams CB, *et al.*, 2017, Polymer structure-property requirements for stereolithographic 3D printing of soft tissue engineering scaffolds. *Biomaterials*, 140(2017): 170–188.
<https://doi.org/10.1016/j.biomaterials.2017.06.005>
 21. Hwa LC, Rajoo S, Noor AM, *et al.*, 2017, Recent advances in 3D printing of porous ceramics: A review. *Curr Opin Solid State Mater Sci*, 21(6): 323–347.
<https://doi.org/10.1016/j.cossms.2017.08.002>
 22. Kuang X, Wu JT, Chen KJ, *et al.*, 2019, Grayscale digital light processing 3D printing for highly functionally graded materials. *Sci Adv*, 5(5): eaav5790.
<https://doi.org/10.1126/sciadv.aav5790>
 23. Shao HF, Ke XR, Liu A, *et al.*, 2017, Bone regeneration in 3D printing bioactive ceramic scaffolds with improved tissue/material interface pore architecture in thin-wall bone defect. *Biofabrication*, 9(2): 12.
<https://doi.org/10.1088/1758-5090/aa663c>
 24. Butscher A, Bohner M, Hofmann S, *et al.*, 2011, Structural and material approaches to bone tissue engineering in powder-based three-dimensional printing. *Acta Biomater*, 7(3): 907–920.
<https://doi.org/10.1016/j.actbio.2010.09.039>
 25. Mousavi S, Howard D, Zhang F, *et al.*, 2020, Direct 3D printing of highly anisotropic, flexible, constriction-resistive sensors for multidirectional proprioception in soft robots. *ACS Appl Mater Interfaces*, 12(13): 15631–15643.
<https://doi.org/10.1021/acsami.9b21816>
 26. Huang K, Dong S, Yang J, *et al.*, 2019, Three-dimensional printing of a tunable graphene-based elastomer for strain sensors with ultrahigh sensitivity. *Carbon*, 143(2019): 63–72.
<https://doi.org/10.1016/j.carbon.2018.11.008>
 27. Jiang Z, Diggel B, Tan ML, *et al.*, 2020, Extrusion 3D printing of polymeric materials with advanced properties. *Adv Sci*, 7(17): 2001379.

- <https://doi.org/10.1002/advs.202001379>
28. Nan B, Galindo-Rosales FJ, Ferreira JMF, 2020, 3D printing vertically: Direct ink writing free-standing pillar arrays. *Mater Today*, 35(2020): 16–24.
<https://doi.org/10.1016/j.mattod.2020.01.003>
29. Lewis JA, 2006, Direct ink writing of 3D functional materials. *Adv Funct Mater*, 16(17): 2193–2204.
<https://doi.org/10.1002/adfm.200600434>
30. Ravichandran D, Xu W, Kakarla M, *et al.*, 2021, Multiphase direct ink writing (MDIW) for multilayered polymer/nanoparticle composites. *Addit Manuf*, 47(2021): 102322.
<https://doi.org/10.1016/j.addma.2021.102322>
31. Nommeots-Nomm A, Lee PD, Jones JR, 2018, Direct ink writing of highly bioactive glasses. *J Eur Ceram Soc*, 38(3): 837–844.
<https://doi.org/10.1016/j.jeurceramsoc.2017.08.006>
32. He YF, Zhang F, Saleh E, *et al.*, 2017, A tripropylene glycol diacrylate-based polymeric support ink for material jetting. *Addit Manuf*, 16(2017): 153–161.
<https://doi.org/10.1016/j.addma.2017.06.001>
33. Brunello G, Sivoletta S, Meneghello R, *et al.*, 2016, Powder-based 3D printing for bone tissue engineering. *Biotechnol Adv*, 34(5): 740–753.
<https://doi.org/10.1016/j.biotechadv.2016.03.009>
34. Miyanaji H, Zhang S, Yang L, 2018, A new physics-based model for equilibrium saturation determination in binder jetting additive manufacturing process. *Int J Mach Tools Manuf*, 124(2018): 1–11.
<https://doi.org/10.1016/j.ijmachtools.2017.09.001>
35. Zhou Z, Lennon A, Buchanan F, *et al.*, 2020, Binder jetting additive manufacturing of hydroxyapatite powders: Effects of adhesives on geometrical accuracy and green compressive strength. *Addit Manuf*, 36(2020):101645.
<https://doi.org/10.1016/j.addma.2020.101645>
36. Du YY, Liu HM, Yang Q, *et al.*, 2017, Selective laser sintering scaffold with hierarchical architecture and gradient composition for osteochondral repair in rabbits. *Biomaterials*, 137(2017): 37–48.
<https://doi.org/10.1016/j.biomaterials.2017.05.021>
37. Wu H, Wang O, Tian Y, *et al.*, 2020, Selective laser sintering-based 4D printing of magnetism-responsive grippers. *ACS Appl Mater Interfaces*, 13(11): 12679–12688.
<https://doi.org/10.1021/acsami.0c17429>
38. Warnke PH, Douglas T, Wollny P, *et al.*, 2009, Rapid prototyping: Porous titanium alloy scaffolds produced by selective laser melting for bone tissue engineering. *Tissue Eng Part C-Methods*, 15(2): 115–124.
<https://doi.org/10.1089/ten.tec.2008.0288>
39. Han CJ, Yan CZ, Wen SF, *et al.*, 2017, Effects of the unit cell topology on the compression properties of porous Co-Cr scaffolds fabricated via selective laser melting. *Rapid Prototyp J*, 23(1): 16–27.
<https://doi.org/10.1108/rpj-08-2015-0114>
40. Xiong Y-Z, Gao R-N, Zhang H, *et al.*, 2020, Rationally designed functionally graded porous Ti6Al4V scaffolds with high strength and toughness built via selective laser melting for load-bearing orthopedic applications. *J Mech Behav Biomed Mater*, 104(2020): 103673.
<https://doi.org/10.1016/j.jmbbm.2020.103673>
41. Liang HX, Yang YW, Xie DQ, *et al.*, 2019, Trabecular-like Ti-6Al-4V scaffolds for orthopedic: Fabrication by selective laser melting and in vitro biocompatibility. *J Mater Sci Technol*, 35(7): 1284–1297.
<https://doi.org/10.1016/j.jmst.2019.01.012>
42. Kinstlinger IS, Saxton SH, Calderon GA, *et al.*, 2020, Generation of model tissues with dendritic vascular networks via sacrificial laser-sintered carbohydrate templates. *Nat Biomed Eng*, 4(9): 916–932.
<https://doi.org/10.1038/s41551-020-0566-1>
43. Mao M, Qu X, Zhang Y, *et al.*, 2023, Leaf-venation-directed cellular alignment for macroscale cardiac constructs with tissue-like functionalities. *Nat Commun*, 14(1): 2077.
<https://doi.org/10.1038/s41467-023-37716-1>
44. Brassard JA, Nikolaev M, Hübscher T, *et al.*, 2021, Recapitulating macro-scale tissue self-organization through organoid bioprinting. *Nat Mater*, 20(1): 22–29.
<https://doi.org/10.1038/s41563-020-00803-5>
45. Koons GL, Diba M, Mikos AG, 2020, Materials design for bone-tissue engineering. *Nat Rev Mater*, 5(8): 584–603.
<https://doi.org/10.1038/s41578-020-0204-2>
46. Liu H, Du Y, St-Pierre J-P, *et al.*, 2020, Bioenergetic-active materials enhance tissue regeneration by modulating cellular metabolic state. *Sci Adv*, 6(13): eaay7608.
<https://doi.org/10.1126/sciadv.aay7608>
47. McDermott Anna M, Herberg S, Mason Devon E, *et al.*, 2019, Recapitulating bone development through engineered mesenchymal condensations and mechanical cues for tissue regeneration. *Sci Transl Med*, 11(495): eaav7756.
<https://doi.org/10.1126/scitranslmed.aav7756>
48. Saba P, Melnyk R, Holler T, *et al.*, 2021, Comparison of multi-parametric MRI of the prostate to 3D prostate computer aided designs and 3D-printed prostate models for pre-operative planning of radical prostatectomies: A pilot study. *Urology*, 158(2021): 150–155.

- <https://doi.org/10.1016/j.urology.2021.08.031>
49. Chandak P, Byrne N, Lynch H, *et al.*, 2018, Three-dimensional printing in robot-assisted radical prostatectomy - an Idea, Development, Exploration, Assessment, Long-term follow-up (IDEAL) Phase 2a study. *BJU Int*, 122(3): 360–361.
<https://doi.org/10.1111/bju.14189>
50. Ebbing J, Jäderling F, Collins JW, *et al.*, 2018, Comparison of 3D printed prostate models with standard radiological information to aid understanding of the precise location of prostate cancer: A construct validation study. *PLoS One*, 13(6): e0199477.
<https://doi.org/10.1371/journal.pone.0199477>
51. Cacciamani GE, Okhunov Z, Meneses AD, *et al.*, 2019, Impact of three-dimensional printing in urology: state of the art and future perspectives. A systematic review by ESUT-YAUWP Group. *Eur Urol*, 76(2): 209–221.
<https://doi.org/10.1016/j.eururo.2019.04.044>
52. Ghazi AE, Teplitz BA, 2020, Role of 3D printing in surgical education for robotic urology procedures. *Transl Androl Urol*, 9(2): 931–941.
<https://tau.amegroups.com/article/view/35484>
53. del Junco M, Okhunov Z, Yoon R, *et al.*, 2014, Development and initial porcine and cadaver experience with three-dimensional printing of endoscopic and laparoscopic equipment. *J Endourol*, 29(1): 58–62.
<https://doi.org/10.1089/end.2014.0280>
54. Park C-J, Kim H-W, Jeong S, *et al.*, 2015, Anti-reflux ureteral stent with polymeric flap valve using three-dimensional printing: An in vitro study. *J Endourol*, 29(8): 933–938.
<https://doi.org/10.1089/end.2015.0154>
55. Lee J, Sung J, Ki JJ, *et al.*, 2022, 3D-printing-assisted extraluminal anti-reflux diodes for preventing vesicoureteral reflux through double-J stents. *Int J Bioprint*, 8(2): 549.
<https://doi.org/10.18063/ijb.v8i2.549>
56. Yoon J, Singh NK, Jang J, *et al.*, 2022, 3D bioprinted in vitro secondary hyperoxaluria model by mimicking intestinal-oxalate-malabsorption-related kidney stone disease. *Appl Phys Rev*, 9(4): 041408.
<https://doi.org/10.1063/5.0087345>
57. Pichler R, Rizzo L, Tröndle K, *et al.*, 2022, Tuning the 3D microenvironment of reprogrammed tubule cells enhances biomimetic modeling of polycystic kidney disease. *Biomaterials*, 291(2022): 121910.
<https://doi.org/10.1016/j.biomaterials.2022.121910>
58. Liu C, Campbell SB, Li J, *et al.*, 2022, High throughput omnidirectional printing of tubular microstructures from elastomeric polymers. *Adv Healthc Mater*, 11(23): 2201346.
<https://doi.org/10.1002/adhm.202201346>
59. Kim JH, Choi J, Kim M, *et al.*, 2022, Immunotherapeutic effects of recombinant Bacillus Calmette–Guérin containing sic gene in ex vivo and in vivo bladder cancer models. *Investig Clin Urol*, 63(2): 228–237.
<https://doi.org/10.4111/icu.20210425>
60. Lee S, Kim JH, Kang SJ, *et al.*, 2022, Customized multilayered tissue-on-a-chip (MToC) to simulate Bacillus Calmette–Guérin (BCG) immunotherapy for bladder cancer treatment. *BioChip J*, 16(1): 67–81.
<https://doi.org/10.1007/s13206-022-00047-2>
61. Chae S, Kim J, Yi H-G, *et al.*, 2022, 3D bioprinting of an in vitro model of a biomimetic urinary bladder with a contract-release system. *Micromachines*, 13(2): 277.
<https://doi.org/10.3390/mi13020277>
62. Wu D, Berg J, Arlt B, *et al.*, 2022, Bioprinted cancer model of neuroblastoma in a renal microenvironment as an efficiently applicable drug testing platform. *Int J Mol Sci*, 23(1): 122.
<https://doi.org/10.3390/ijms23010122>
63. Sobreiro-Almeida R, Gomez-Florit M, Quinteira R, *et al.*, 2021, Decellularized kidney extracellular matrix bioinks recapitulate renal 3D microenvironment in vitro. *Biofabrication*, 13(4): 17.
<https://doi.org/10.1088/1758-5090/ac0fca>
64. Kim JH, Lee S, Kang SJ, *et al.*, 2021, Establishment of three-dimensional bioprinted bladder cancer-on-a-chip with a microfluidic system using Bacillus Calmette-Guerin. *Int J Mol Sci*, 22(16): 17.
<https://doi.org/10.3390/ijms22168887>
65. Trondle K, Rizzo L, Pichler R, *et al.*, 2021, Scalable fabrication of renal spheroids and nephron-like tubules by bioprinting and controlled self-assembly of epithelial cells. *Biofabrication*, 13(3): 16.
<https://doi.org/10.1088/1758-5090/abe185>
66. Serex L, Sharma K, Rizov V, *et al.*, 2021, Microfluidic-assisted bioprinting of tissues and organoids at high cell concentrations. *Biofabrication*, 13(2): 025006.
<https://doi.org/10.1088/1758-5090/abca80>
67. Lawlor KT, Vanslambrouck JM, Higgins JW, *et al.*, 2021, Cellular extrusion bioprinting improves kidney organoid reproducibility and conformation. *Nat Mater*, 20(2): 260–271.
<https://doi.org/10.1038/s41563-020-00853-9>
68. Xie R, Korolj A, Liu C, *et al.*, 2020, h-FIBER: Microfluidic topographical hollow fiber for studies of glomerular filtration barrier. *ACS Central Sci*, 6(6): 903–912.
<https://doi.org/10.1021/acscentsci.9b01097>
69. Sämfors S, Karlsson K, Sundberg J, *et al.*, 2019, Biofabrication of bacterial nanocellulose scaffolds with complex vascular structure. *Biofabrication*, 11(4): 045010.

- <https://doi.org/10.1088/1758-5090/ab2b4f>
70. Ali M, Pr AK, Yoo JJ, *et al.*, 2019, A photo-crosslinkable kidney ECM-derived bioink accelerates renal tissue formation. *Adv Healthc Mater*, 8(7): 1800992.
<https://doi.org/10.1002/adhm.201800992>
71. Lin NYC, Homan KA, Robinson SS, *et al.*, 2019, Renal reabsorption in 3D vascularized proximal tubule models. *Proc Natl Acad Sci*, 116(12): 5399–5404.
<https://doi.org/10.1073/pnas.1815208116>
72. Jansen K, Castilho M, Aarts S, *et al.*, 2019, Fabrication of kidney proximal tubule grafts using biofunctionalized electrospun polymer scaffolds. *Macromol Biosci*, 19(2): 1800412.
<https://doi.org/10.1002/mabi.201800412>
73. Imamura T, Shimamura M, Ogawa T, *et al.*, 2018, Biofabricated structures reconstruct functional urinary bladders in radiation-injured rat bladders. *Tissue Eng Part A*, 24(21–22): 1574–1587.
<https://doi.org/10.1089/ten.tea.2017.0533>
74. Pi Q, Maharjan S, Yan X, *et al.*, 2018, Digitally tunable microfluidic bioprinting of multilayered cannular tissues. *Adv Mater*, 30(43): 1706913.
<https://doi.org/10.1002/adma.201706913>
75. Liang Q, Gao F, Zeng Z, *et al.*, 2020, Coaxial scale-up printing of diameter-tunable biohybrid hydrogel microtubes with high strength, perfusability, and endothelialization. *Adv Funct Mater*, 30(43): 2001485.
<https://doi.org/10.1002/adfm.202001485>
76. Xu Z, Fan C, Zhang Q, *et al.*, 2021, A self-thickening and self-strengthening strategy for 3D printing high-strength and antistiffening supramolecular polymer hydrogels as meniscus substitutes. *Adv Funct Mater*, 31(18): 2100462.
<https://doi.org/10.1002/adfm.202100462>
77. Gong J, Schuurmans CCL, Genderen AMv, *et al.*, 2020, Complexation-induced resolution enhancement of 3D-printed hydrogel constructs. *Nat Commun*, 11(1): 1267.
<https://doi.org/10.1038/s41467-020-14997-4>
78. Park S, Yuk H, Zhao R, *et al.*, 2021, Adaptive and multifunctional hydrogel hybrid probes for long-term sensing and modulation of neural activity. *Nat Commun*, 12(1): 3435.
<https://doi.org/10.1038/s41467-021-23802-9>
79. Fan W, Shan C, Guo H, *et al.*, 2022, Dual-gradient enabled ultrafast biomimetic snapping of hydrogel materials. *Sci Adv*, 5(4): eaav7174.
<https://doi.org/10.1126/sciadv.aav7174>
80. Duraivel S, Laurent D, Rajon DA, *et al.*, 2023, A silicone-based support material eliminates interfacial instabilities in 3D silicone printing. *Science*, 379(6638): 1248–1252.
<https://doi.org/10.1126/science.ade4441>
81. Zhao S, Siqueira G, Drdova S, *et al.*, 2020, Additive manufacturing of silica aerogels. *Nature*, 584(7821): 387–392.
<https://doi.org/10.1038/s41586-020-2594-0>
82. Xu J, Zhang X, Liu Y, *et al.*, 2020, Selective coaxial ink 3D printing for single-pass fabrication of smart elastomeric foam with embedded stretchable sensor. *Addit Manuf*, 36(2020): 101487.
<https://doi.org/10.1016/j.addma.2020.101487>
83. Cooke MN, Fisher JP, Dean D, *et al.*, 2003, Use of stereolithography to manufacture critical-sized 3D biodegradable scaffolds for bone ingrowth. *J Biomed Mater Res Part B-Appl Biomater*, 64B(2): 65–69.
<https://doi.org/10.1002/jbm.b.10485>
84. Wang Z, Huang CZ, Wang J, *et al.*, 2019, Development of a novel aqueous hydroxyapatite suspension for stereolithography applied to bone tissue engineering. *Ceram Int*, 45(3): 3902–3909.
<https://doi.org/10.1016/j.ceramint.2018.11.063>
85. Caprioli M, Roppolo I, Chiappone A, *et al.*, 2021, 3D-printed self-healing hydrogels via digital light processing. *Nat Commun*, 12(1): 1–9.
<https://doi.org/10.1038/s41467-021-22802-z>
86. Chen Z, Yang M, Ji M, *et al.*, 2021, Recyclable thermosetting polymers for digital light processing 3D printing. *Mater Des*, 197(2021): 109189.
<https://doi.org/10.1016/j.matdes.2020.109189>
87. Mazzoli A, Ferretti C, Gigante A, *et al.*, 2015, Selective laser sintering manufacturing of polycaprolactone bone scaffolds for applications in bone tissue engineering. *Rapid Prototyp J*, 21(4): 386–392.
<https://doi.org/10.1108/rpj-04-2013-0040>
88. Liu C, Yan D, Tan J, *et al.*, 2020, Development and experimental validation of a hybrid selective laser melting and CNC milling system. *Addit Manuf*, 36(2020): 101550.
<https://doi.org/10.1016/j.addma.2020.101550>
89. Hu Y, Chen H, Liang X, *et al.*, 2021, Microstructure and biomechanical properties in selective laser melting of porous metal implants. *3D Print Addit Manuf*, 0(0): 1–12.
<https://doi.org/10.1089/3dp.2021.0150>
90. Buote NJ, Porter I, Dakin GF, 2022, 3D printed cannulas for use in laparoscopic surgery in feline patients: A cadaveric study and case series. *Vet Surg*, n/a(n/a).
<https://doi.org/10.1111/vsu.13849>